Growth-direction-dependent characteristics of Ge-on-insulator by Si-Ge mixing triggered melting growth

Ohta, Y.
Department of Electronics, Kyushu University

Tanaka, T.
Department of Electronics, Kyushu University

Toko, T.
Department of Electronics, Kyushu University

Sadoh, Taizo
Department of Electronics, Kyushu University

他

https://hdl.handle.net/2324/25499

出版情報：Solid-State Electronics. 60 (1), pp.18-21, 2011-06. Elsevier
バージョン：

Growth-Direction-Dependent Characteristics of Ge-on-Insulator by SiGe Mixing Triggered Melting Growth

Y. Ohta, T. Tanaka, K. Toko, T. Sadoh and M. Miyao

Department of Electronics, Kyushu University, 744 Motooka, Fukuoka, 819-0395, Japan

E-mail: sadoh@ed.kyushu-u.ac.jp

Abstract

The lateral liquid-phase epitaxy of Ge-on-insulator (GOI) using Si seeds has been investigated as a function of the Si-seed orientation and the growth direction. Giant single-crystalline GOI structures with ~200 μm length are obtained using Si(100), (110), and (111) seeds. The very long growth is explained on the basis of the solidification temperature gradient due to Si-Ge mixing around the seeding area and the thermal gradient due to the latent heat around the solid/liquid interface at the growth front. In addition, growth with rotating crystal orientations are observed for samples with several growth directions. The rotating growth is explained on the basis of the bonding strength between lattice planes at the growth front. This rotating growth does not occur in any direction for (100) orientated seeds. Based on this finding the mesh-patterned GOI growth with a large area (250μm x 500μm) is demonstrated.

Keywords : Ge, GOI, liquid-phase crystallization,

1. Introduction

The Ge-on-insulator (GOI) is a promising channel materials for the advanced transistors with the very high-speed and low-power consumption [1-3]. In order to obtain GOI structures, various formation techniques, such as wafer bonding [4], oxidation-induced Ge condensation [5], and imprint-induced solid-phase crystallization [6], have been intensively developed. However, these techniques require complex processing or have difficulty in obtaining high-quality GOI structures.

Recently, lateral liquid-phase epitaxy (L-LPE) of Ge layers (length: ~40 μm) on insulator was reported by several research groups [7-10], where Si substrates were used as the crystal seeds for epitaxial growth of Ge layers. We previously succeeded in the giant (~200 μm) growth of GOI by optimizing sample structures and annealing conditions [11-13]. This growth length was one order larger than those reported in the previous works [7-10]. However, the detailed growth features, such as the crystal orientation dependence, have not been clarified. In the present paper, we investigate the effect of crystal orientation of Si seeds on the growth features, and discuss the rotating growth of GOI. In addition, we apply this technique to achieve a large area GOI by using a mesh pattern.

2. Experimental Procedure

In the experiments, Si(100), (110), and (111) substrates covered with thermally grown SiO_2 films (50 nm thickness) were used. The SiO_2 films on the substrates were selectively removed by wet etching to form seeding areas ($150 \times 30\ \mu m^2$). Subsequently, amorphous-Ge (a-Ge) layers (100 nm thickness) were deposited using a solid-source molecular beam epitaxy (MBE) system (base pressure: 5×10^{-11} Torr) at a room temperature, and they were patterned into narrow stripe lines (200 μm length, 3-5 μm width). The sample structure is schematically shown in Fig. 1. Then capping SiO_2 layers (800 nm thickness) were deposited by RF magnetron sputtering. Finally, these samples were heat-treated by rapid thermal annealing (RTA) ($1000^{o}C$, 1 s) with heating and cooling rates of ~40 and ~$10^{o}C$/sec, respectively, to induce liquid-phase epitaxial growth from the seeding areas.

The grown layers were characterized by Nomarski optical microscopy, electron backscattering diffraction (EBSD), and micro-probe (spot size: ~1 μmϕ) Raman scattering spectroscopy. The capping SiO_2 layers were etched off before the EBSD measurements.

3. Results and Discussions

The EBSD images of the samples grown on Si(100), (110), and (111) substrates are shown in Fig.2, where the growth directions are shown in the figures. It is found that giant single crystalline Ge stripes (length: 200 μm) with crystal orientations identical to those of Si seeds are realized on the

SiO_2 layers using Si(100) and (110) seeding substrates. On the other hand, for the Si(111) substrate, the crystal orientation of the giant GOI structure grown along the <011> direction is (111), though that along the <121> direction gradually changes from (111) to (100). These results clearly show that crystal growth is initiated at Si seeding areas and propagates laterally over SiO_2 films for all samples.

In order to evaluate the crystal quality and the Si fraction in laterally-grown regions, micro-probe Raman spectra were measured as a function of the distance from the seeding edges. The full-width at half maximum (FWHM) of the Raman peaks at 296.8 cm^{-1} due to Ge-Ge bonds for the sample with the Si(100) seeding substrate grown to the <011> direction, shown in Fig. 2 (a), is summarized in Fig. 3(a), where FWHM obtained from a single crystalline Ge bulk wafer is also shown for comparison. The FWHM values in the seeding area are about 4-5 cm^{-1}, which is wider than that of single crystalline Ge (3.2 cm^{-1}). However, almost equal values (~3.3 cm^{-1}) to single-crystalline Ge are obtained from the L-LPE area, indicating the high crystal quality. The FWHM values obtained from the L-LPE areas of the samples shown in Figs. 2(b)-2(f) were also ~3.3 cm^{-1}. Although a grain boundary (GB) existed in the sample shown in Fig. 2(f), the small FWHM was obtained, which was probably because that the Raman peak was not broadened due to the very large grains with very high crystallinity.

The Si fractions in the grown layers were evaluated from the intensities of Raman peaks due to Ge-Ge (296.8 cm^{-1}) and Si-Ge bonds (380.9 cm^{-1}) [11,14]. The result is shown in Fig. 3(b) as a function of the distance from the seeding edge. It is found that the Si fractions in the seeding area and the seeding edge on SiO_2 are 8% and 4%, respectively. It gradually decreases along the growth direction and reaches to zero, where lateral growth length exceeds 70 μm. Consequently, pure single crystalline Ge is obtained in the large region of 70 to 200 μm from the seeding edge.

The possible candidates of the driving force to initiate L-LPE of Ge on SiO_2 layers are the thermal flow from the liquid SiGe or Ge region to the Si substrate through seeding window or the increase in the solidification temperature due to Si-Ge mixing. However, the result of an additional experiment on quartz substrates employing poly-Si seeds, which suppresses thermal flow from the liquid SiGe or Ge regions to the substrates through seeding windows, indicated that Si-Ge mixing at seeding areas is the most important force to trigger the L-LPE [11].

In order to explain such a giant lateral growth of pure Ge obtained in the region far from the seeding area (> 70 μm), another force should be considered, because the gradient of the Si fraction does not exist in this region. The latent heat of solidification at the solid-liquid interface is the important driving force to realize the giant growth. In the cooling process after RTA, the temperature of the solid-Ge rapidly falls with time. However, the molten-Ge tends to keep a constant melting-temperature due to latent heat. Consequently, a thermal gradient is automatically formed at the growth front, which realizes the continuous L-LPE [11]. The maximum growth length obtained in our experiments is limited by the sample structures, where a-Ge stripe patterns with 200 μm length are employed. Thus, we expect that very long lateral growth over 200 μm is possible by this L-LPE method.

From detailed analysis of the EBSD data, it was found that the crystal orientations of the growth directions in-plane to the sample surfaces did not change for all samples grown using Si(111) seeding substrates, though the crystal orientation of the surface of the Ge layer grown along to the <121> direction gradually changed, as shown in Fig. 2(f). These results show that rotating growth occurs for the sample with the Si(111) seeding substrate grown along <121>. On the other hand, such a rotating growth was not observed along <011> even though the use of the Si(111) seed, as shown in Fig. 2(e).

In order to reveal the details of the rotating growth, the change in the crystal orientation perpendicular to the film plane was investigated as a function of the distance from the seeding edge. The results are summarized in Fig. 4(a). It is found that the rotation angle increases from 0^o to 25^o with increasing distance from 0 to about 23 μm. At the distance of about 23 μm, the rotation angle abruptly increases to 60^o, which corresponds to the (100) orientation. The abrupt increase in the rotation angle coincides with formation of a grain boundary (GB), as shown in Fig. 2(f).

We further investigated the rotation of the crystal orientations of the film planes for various growth directions with the Si(111) seeding substrate.

The maximum rotation angles before the grain boundary formation are summarized in Fig. 4(b). It is found that the rotation angle changes with a 60^o period. Namely the rotating growth significantly occurs along the <121> and its equivalent directions, while it is scarcely observed along the <011> and its equivalent directions. The period of 60^o well agrees with that of crystal symmetry. It is noted that mostly observed orientations of the surfaces of the Ge layers after grain boundary formation were (100) and (110), which suggests that Ge layers tend to orient to the (100) and (110) orientations compared with the (111) orientation on SiO_2 films. It is reported that the orientation tendency of poly-Si grown by laser annealing strongly depends on the process conditions [15].

Although the Ge(111)/SiO_2 seems to be energetically unstable, the rotating occurs for growth along the specific crystal directions. This suggests that the occurrence of the rotating growth depends on the crystallographic properties of Ge, such as bonding strength between lattice planes perpendicular to the growth directions. As revealed from the orientation dependence of the cleavage, the bonding strength of lattice planes is the weakest for (111). Since the (111) planes inclined with 30^o compose the growth front toward the <121> direction, it is speculated that the lattice planes at the growth front can easily rotate by slipping between the (111) planes for growth along <121>. Thus, the growth direction dependence of the rotating growth can be qualitatively explained on the basis of the bonding strength between lattice planes perpendicular to the growth directions. This rotating growth was not observed for samples grown on Si(100) with any growth directions, where the growth directions near <111> did not exist on the Si(100) plane.

In order to realize a large area GOI, we examined the growth of Ge layers with mesh-patterns. Since the rotating growth does not occur for Ge layers on Si(100), the (100) orientation is expected to be applicable to achieve a large area Ge mesh on insulator, where lateral growth propagate along various direction. A detailed schematic structure of the Ge mesh-pattern and EBSD images after RTA are shown in Fig.5. Interestingly, the whole Ge regions are uniformly orientated to the (100) direction. As a result, a large area GOI mesh with the (100) orientation has been realized.

4. Conclusion

We have demonstrated the giant liquid-phase epitaxial growth of single-crystalline Ge(100), (110), and (111) layers (length: 200 μm) on SiO_2 films using Si(100), (110), and (111) seeding substrates, respectively. The giant growth is triggered by the solidification temperature gradient due to Si-Ge mixing and assisted by the temperature gradient due to latent heat. Moreover, rotating growth of Ge layers occurred for samples with the Si(111) seeds. The phenomena were observed for growth toward around <121> and its equivalent directions with a 60^{o} period. This phenomenon is quantitatively explained on the basis of the bonding strength between lattice planes of the growth front. This, rotation growth does not occurs for Ge(100) in any directions. Based on this finding, we proposed mesh-patterned GOI using Si(100) seeding substrates, and succeeded in growth of a large area GOI(100) (250μm x 500μm) mesh without crystal rotation.

.

Acknowledgements

A part of this work was supported by Semiconductor Technology Academic Research Center (STARC) and a Grant-in-Aid for Scientific Research from the Ministry of Education, Culture, Sports, and Technology in Japan.

References

[1] M. Miyao, E. Murakami, H. Etoh, K. Nakagawa, and A. Nishida, J. Cryst. Growth Vol. 111, p. 912, 1991.

[2] M. Miyao and K. Nakagawa, Jpn. J. Appl. Phys. Vol. 33, p. 3791 1994.

[3] G. Taradchi, A. J. Pitera, and E. A. Fitzgerald, Solid-State Electron. Vol. 48, p. 1297, 2004.

[4] C. H. Huang, M. Y. Yang, A. Chin, W. J. Chen, C. X. Zhu, B. J. Cho, M-F. Li, and D. L. Kwong, 2003 Symp. VLSI Technology, Dig. Tech. Pap. p. 119, 2003.

[5] S. Nakaharai, T. Tezuka, N. Sugiyama, Y. Moriyama, and S. Takagi, Appl. Phys. Lett. Vol. 83, p.3516, 2003.

[6] K. Toko, H. Kanno, A. Kenjo, T. Sadoh, T. Asano, and M. Miyao, Appl. Phys. Lett. Vol. 91, p. 042111, 2007.

[7] Y. Liu, M. D. Deal, and D. Plummer, Appl. Phys. Lett. Vol. 84, p. 2563, 2004.

[8] D. J. Tweet, J. J. Lee, J. S. Maa, and S. T. Hsu, Appl. Phys. Lett. Vol. 87, p. 141908, 2005.

[9] F. Gao, S. J. Lee, S. Balakumar, A. Du, Y-L. Foo, and D-L. Kwong, Thin Solid Films Vol. 504, p. 69, 2006.

[10] S. Balakumar, M. M. Roy, B. Ramamurthy, C. H. Tung, G. Fei, S. Tripathy, C. Dongzhi, R. Kumar, N. Balasubramanian, and D. L. Kwog, Electrochem. Solid-State Lett. Vol. 9, p. G158, 2006.

[11] M. Miyao, T. Tanaka, K. Toko, and M. Tanaka, Appl. Phys. Express

Vol. 2, p. 045503, 2009.

[12] M. Miyao, K. Toko, T, Tanaka, and T, Sadoh, Appl. Phys. Lett. 95, 022115 (2009)

[13] T. Tanaka, K. Toko, T, Sadoh, and M. Miyao, Appl. Phys. Express vol. 3, p. 031301 (2010)

[14] P. M. Mooney, F. H. Dacol, J. C. Tsang, and J. O. Chu, Appl. Phys. Lett. Vol. 62, p. 2069, 1993.

[15] M. W. Geis, D. C. Flanders, and H. I. Smith, Appl. Phys. Lett. Vol. 35, p. 71, 1979.

Figure captions

Fig.1 Schematic sample structure before SiO_2 capping.

Fig.2 EBSD images for samples grown with Si(100) (a,b), Si(110) (c,d), and Si(111) seeding substrates (e,f)..

Fig.3 FWHM of Raman peak due to Ge-Ge bonds (a), and Si fraction distribution in Ge layers (b).

Fig.4 Rotation angle as a function of the distance from seeding edge (a) and growth direction (b).

Fig. 5 Schematic Ge mesh-pattern (a), and EBSD images near the seeding edge (b) and end of the growth (c). The Si(100) substrate was employed as the seed.

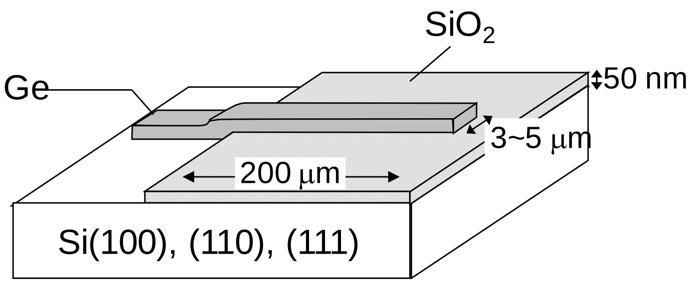

Fig. 1 Y. Ohta

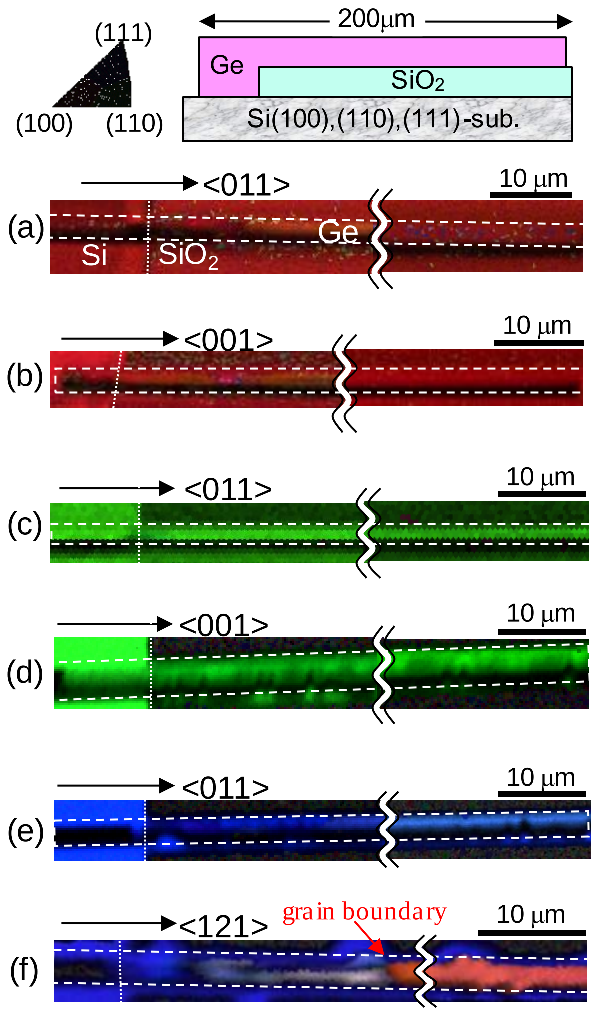

(111)
(100)
(110)
200μm
Ge
SiO2
Si(100),(110),(111)-sub.
(a)
<011>
10 μm
Si
SiO2
Ge
(b)
<001>
10 μm
(c)
<011>
10 μm
(d)
<001>
10 μm
(e)
<011>
10 μm
(f)
<121>
grain boundary
10 μm

Fig. 2 Y. Ohta

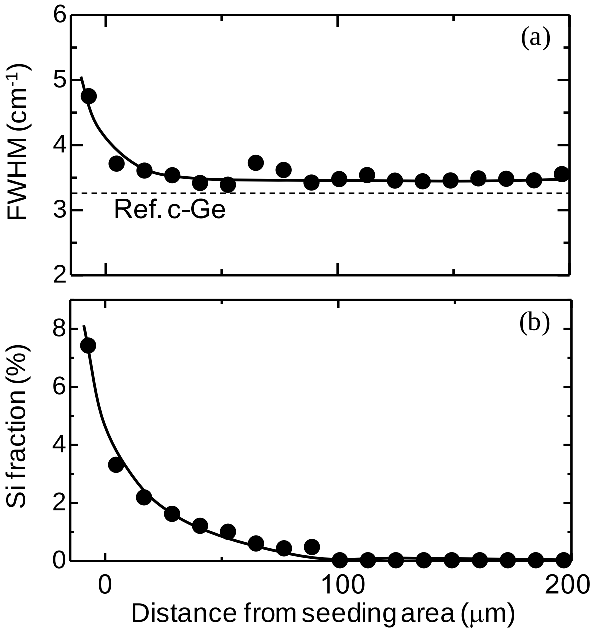

(a)
FWHM (cm-1)
6
5
4
3
2
Ref. c-Ge
(b)
Si fraction (%)
8
6
4
2
0
0
100
200
Distance from seeding area (μm)

Fig. 3 Y. Ohta

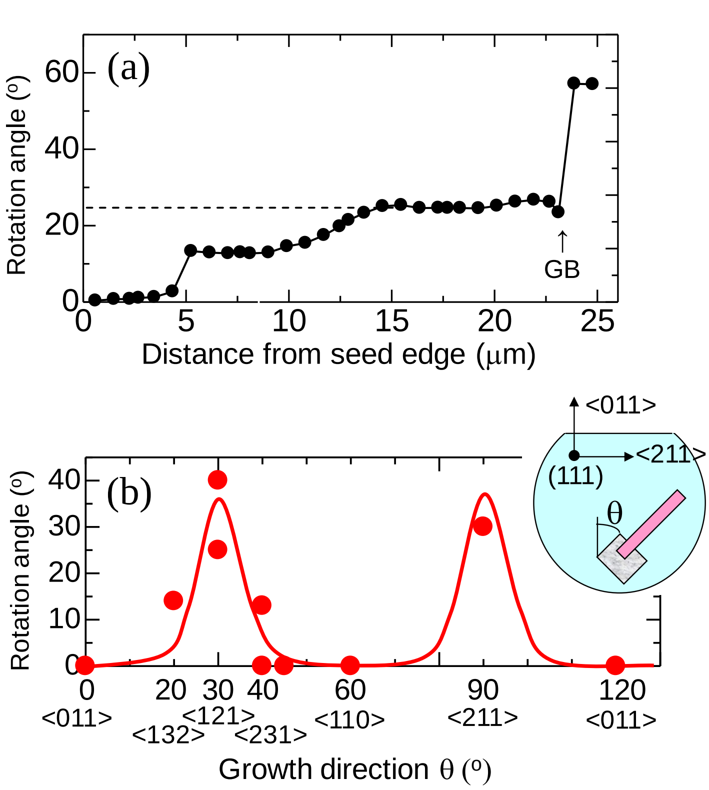
(a)
Rotation angle (º)
0
20
40
60
GB
0
5
10
15
20
25
Distance from seed edge (μm)
(b)
Rotation angle (º)
0
10
20
30
40
<011>
<211>
(111)
θ
0
20
30
40
60
90
120
<011>
<132>
<121>
<231>
<110>
<211>
<011>
Growth direction θ (º)

Fig.4 Y.Ohta

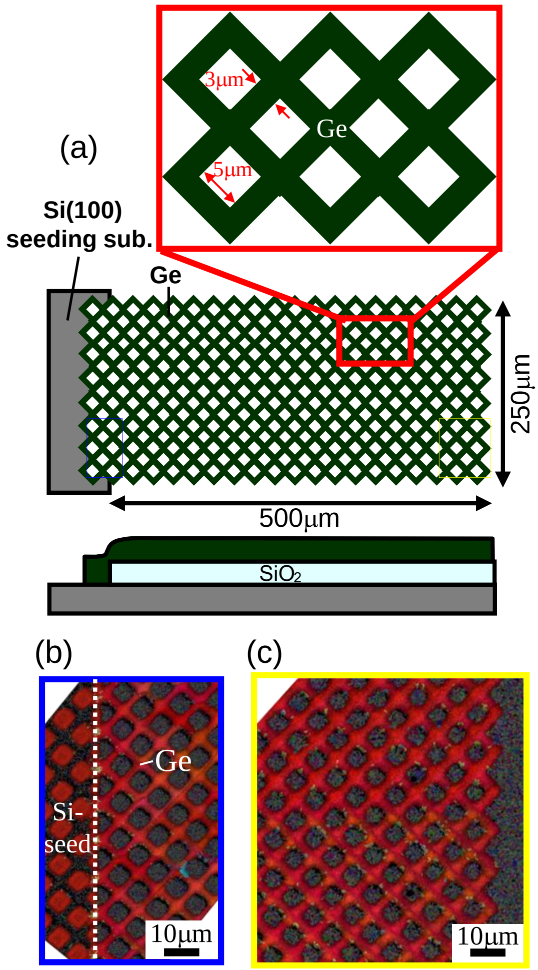
(a)
3μm
Ge
5μm
Si(100)
seeding sub.
Ge
250μm
500μm
SiO2
(b)
-Ge
Si-
seed
10μm
(c)
10μm

Fig.5 Y.Ohta